Studies on Membrane Formation Mechanism by the Light Transmission Technique. I

Ji Hua Hao, Shichang Wang

School of Chemical Engineering, Tianjin University, Tianjin 300072, People's Republic of China

Received 26 October 2001; accepted 13 February 2002

ABSTRACT: New parameters, light transmission rate and minimum light transmissions, are proposed. These two parameters reflect the characteristics of the membrane-forming system and the formation process of the membranes by phase inversion. The relationship between the light transmission and the porous structure of the membrane can be explained by the geometrical optics principles. Variation of the two parameters combining Reuvers's phase separation theory provided a convenient analytical method to predict effectively membrane morphologies. © 2002 Wiley Periodicals, Inc. J Appl Polym Sci 87: 174–181, 2003

Key words: membranes

INTRODUCTION

Phase inversion is the most important process for preparing polymeric membranes. The principal steps involve casting a thin film of homogeneous polymer solution onto a suitable substrate, followed by quenching in a nonsolvent bath to precipitate the membrane film. In some cases, the nonsolvent quench is preceded by a short evaporation period. One brings about phase inversion by bringing the initially thermodynamically stable polymer solution to an unstable state by solvent/nonsolvent exchange during the quench step, which determines the ultimate membrane structure. Because membrane transport properties correlate directly with their morphological structure, the mechanism of formation of these membranes has been the subject of extensive investigation.[1–4] In recent years, significant progress has been made in the mathematical modeling of this process through the application of ternary diffusion theory to the quench step and the combined evaporation and quench steps.[5–9] These models allow the accurate calculation of the diffusion process, which precedes phase separation in terms of measurable transport and thermodynamic parameters. The presence of other phase transitions, such as glass transition, crystallization, and gelation, have also been quantified for their potential role in the structuring mechanism.[10,11] On the other hand, many experimental techniques have been developed to observe and predict the phase separation and morphological structure that occur during membrane formation by phase inversion.

McHugh and Tsay developed methods based on dark ground optics, reflected light illumination, and interface visualization, in combination with video image processing, to monitor the mass transfer and phase separation processes that take place in polymer films during the quench period.[12]

Reuvers and Smolders measured the time it takes before liquid–liquid demixing occurs by light transmission experiments on an immersed casting solution.[13] According to the results, the liquid–liquid demixing process in polymer solutions during membrane formation may proceed in two different ways, delayed demixing and instantaneous demixing, as shown in Figure 1. In case of delayed demixing, there is a certain time interval between the moment of immersion of the polymer solution in a nonsolvent bath and the onset of demixing. As a result, the morphological structure of the membrane comprises a dense and rather thick skin layer supported by a closed-cell sponge-like substructure. This type of membranes exhibits solution-diffusion separation properties, but the fluxes are rather low. The undesirable closed-cell support tends to increase resistance, which leads to low or no selectivity in series with the selective layer.

The morphological structure of the membrane from effectively instantaneous phase separation typically consist of a very thin but microporous skin layer and an open-cell finger or sponge support layer. Such membranes generally show size exclusion capabilities and are useful for microfiltration or ultrafiltration applications. The spinodal decomposition is responsible for the rapid phase separation.

Correspondence to: J. H. Hao, Department of Chemical Engineering, Tulane University, New Orleans, LA 70118-6333 (hao@tulane.edu).

Contract grant sponsor: Ph.D. Research Foundation of the Education Ministry of China.

Journal of Applied Polymer Science, Vol. 87, 174–181 (2003)

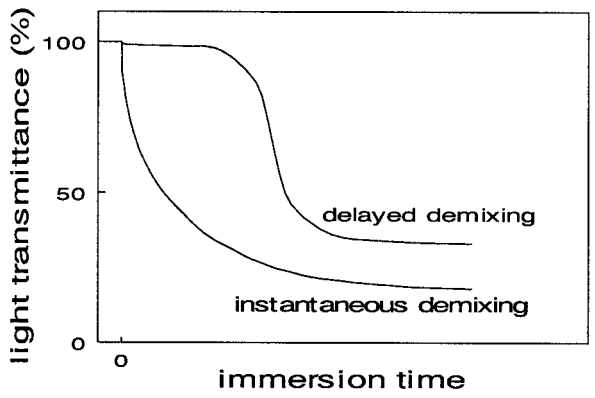

Figure 1 Light transmittances as a function of immersion time.[14]

Van't Hof et al. successfully invented integrally skinned asymmetric hollow-fiber gas-separation membranes with high selectivity by a dual-bath coagulation method, which is a perfect embodiment of Reuvers's theory.[14] Pinnau and Koros explained the coagulant characteristic and morphological structure of the support layer of the integrally skinned asymmetric polysulfone membrane by a dry/wet phase-inversion process using forced-convective evaporation in light of Reuvers's theory.[15] In addition, Reuvers's theory has been used to understand the formation of large finger-like cavities and some other phenomena of membrane formation by phase inversion.[16]

In our laboratory, we made cellulose acetate (CA) membranes with membrane-forming systems of CA–acetone and quench media, such as water, methanol, ethanol, and isopropanol, and observed the phase separation process by a light transmission experiment during precipitation.[17–19] We found that Reuvers's theory was only suitable for part of the experimental results. The morphological structure and the separation performances of the membrane predicted by our light transmission experiment sometimes were contradictory to the morphological structure observed by scanning electron photomicrographs and the measured separation performances. Therefore, in this article, we propose new parameters reflecting the characteristics of the membrane-forming system and the formation process of the membranes: light transmission rate and minimum light transmission. The variation of the two parameters combining Reuvers's theory can be used to explain our experimental results.

EXPERIMENTAL

Membrane preparation

CA was dissolved into acetone. Then, an additive, such as water, was added into the cast solution. All membranes were cast on glass plates of equal nominal thickness at 25°C atmospheric temperature and 55% atmospheric relative humidity and were gelled in a coagulation bath of water after some evaporation time in air.

Gas permeation experiment

Pure gas pressure-normalized fluxes reported in this study were obtained at 25°C for membrane samples of 19.6 cm^2 surface area at a pressure difference of 0.5 MPa. Volumetric gas permeation rates were determined with soap bubble flow meters. The downstream side was always purged with the test gas prior to the permeation measurement.

The feed and permeate compositions of the mixture gas were measured by gas chromatography with a GOW-MAC400 instrument.

Scanning electron microscopy

For structure investigations, we prepared the membranes by cryogenic breaking in liquid nitrogen, followed by the sputtering of a thin layer of gold, and they were examined with an X-650 scanning electron microscope.

Light transmission apparatus and experiments

The system of the light transmission is shown in Figure 2. A light from the light source was focused into a

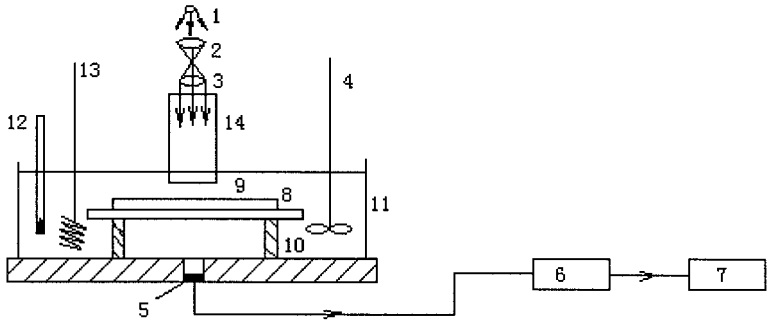

Figure 2 Measurement of the light transmission intensity during an immersion–precipitation process: (1) light source, (2,3) lenses, (4) stirrer, (5) detector, (6) light intensity distributor; (7) recorder, (8) glass plate, (9) membrane solution, (10) light-proof shield, (11) coagulation bath, (12) thermometer, (13) heater, and (14) light-proof cylinder.

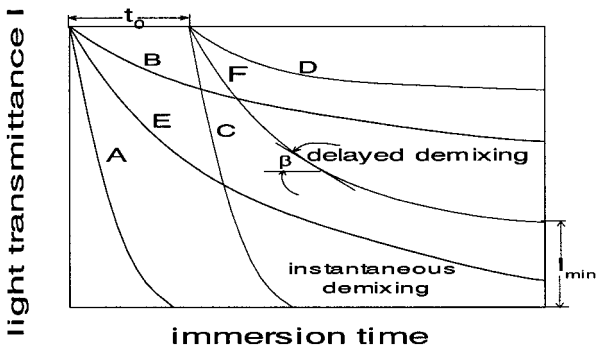

Figure 3 Light transmittance intensity as a function of immersion time and the relative parameters: (A,B,E) instantaneous demixing and (C,D,F) delayed demixing: t_o = delayed demixing time; β = light transmission rate; I_{min} = minimum light transmission.

collimated light beam through a series of lenses (2 and 3). The beam was then directed toward the membrane solution (9) by a light-proof cylinder (14). To prevent the surface scattering caused by surface waves on immersion, we immersed the lightproof cylinder in the coagulation bath. The transmitted beam was transformed into an electrical signal with a detector (5). The electrical signal was amplified by a light intensity distributor and further to recorder (7) where the light transmittance was measured and recorded as a function of time during the immersion of the casting film in the coagulation bath. The temperature in the coagulation bath was 25 ± 1°C controlled by a stirrer (4) and a thermometer (12).

The light transmission experiments were used to measure the phase separation process. At the onset of a phase change, the originally clear membrane solution turned hazy, and as precipitation proceeded, the membrane solution became more and more cloudy until the phase separation was complete. The appearance of optical inhomogenities in the film, as a result of liquid–liquid demixing, caused the light transmittance to decrease.

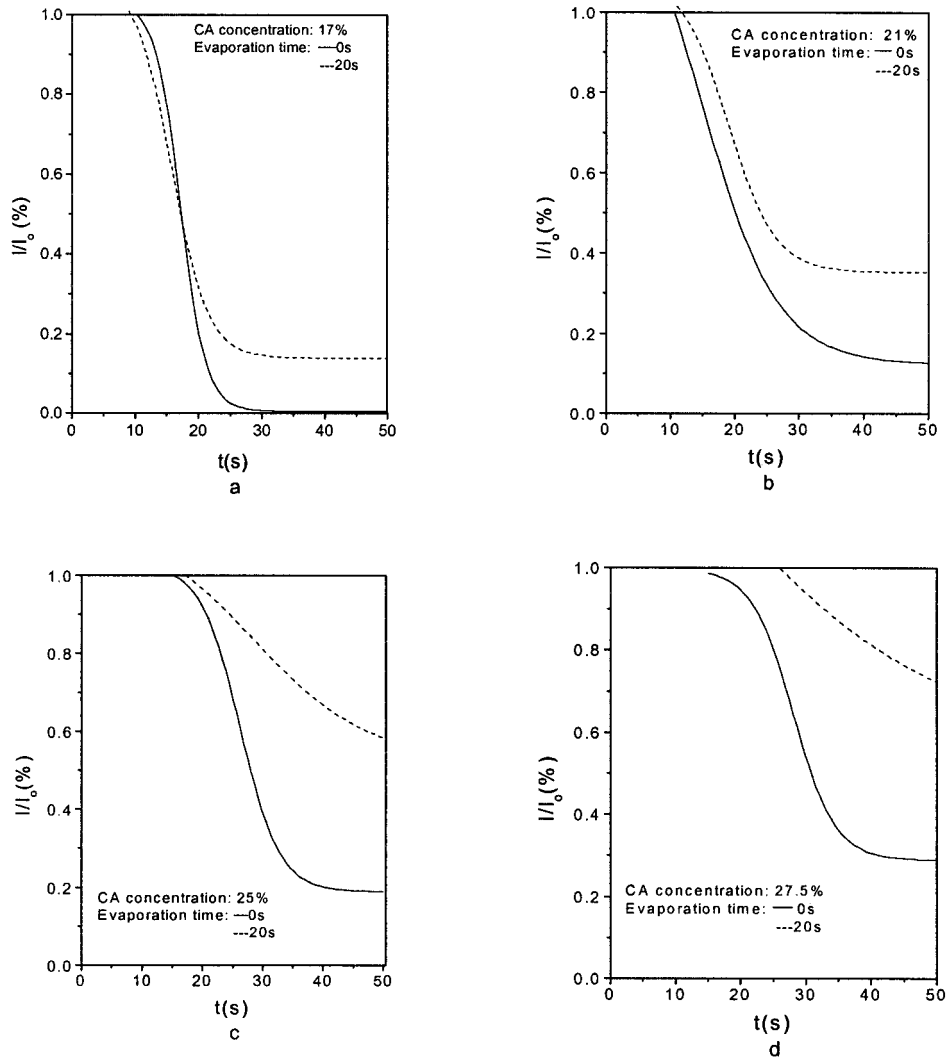

Figure 4 Light transmission–immersion time relationship for the CA–acetone casting solution in a water coagulation bath.

TABLE I
The Effect of the CA Concentration in the Casting Solution[18,19]

CA concentration (%)	Delayed demixing time (s)	CO_2/CH_4 selectivity	Permeability$(P/L)_{CO2} \times 10^5$ cm^3/cm^2-s-cmHg
17	9	5.6	0.06
21	10	7.2	0.12
25	15	13.5	0.08
27	15	22.0	0.06

DEFINITION AND MEANING OF NEW PARAMETERS

To efficiently make use of the light transmission–immersion time curve, which was a simple and direct way to analyze the phase separation of cast membrane during precipitation process, the new parameters were proposed: the rate of light transmission (β; or light transmission intensity) and the minimum light transmission intensity (I_{min}). Several typical parameters are shown in the rate of light transmission–immersion time curves in Figure 3.

Rate of light transmission is defined as the rate of change of light transmission intensity through the membrane (I) at any time during phase inversion process. It can be written as

$$\beta = -dI/dt$$

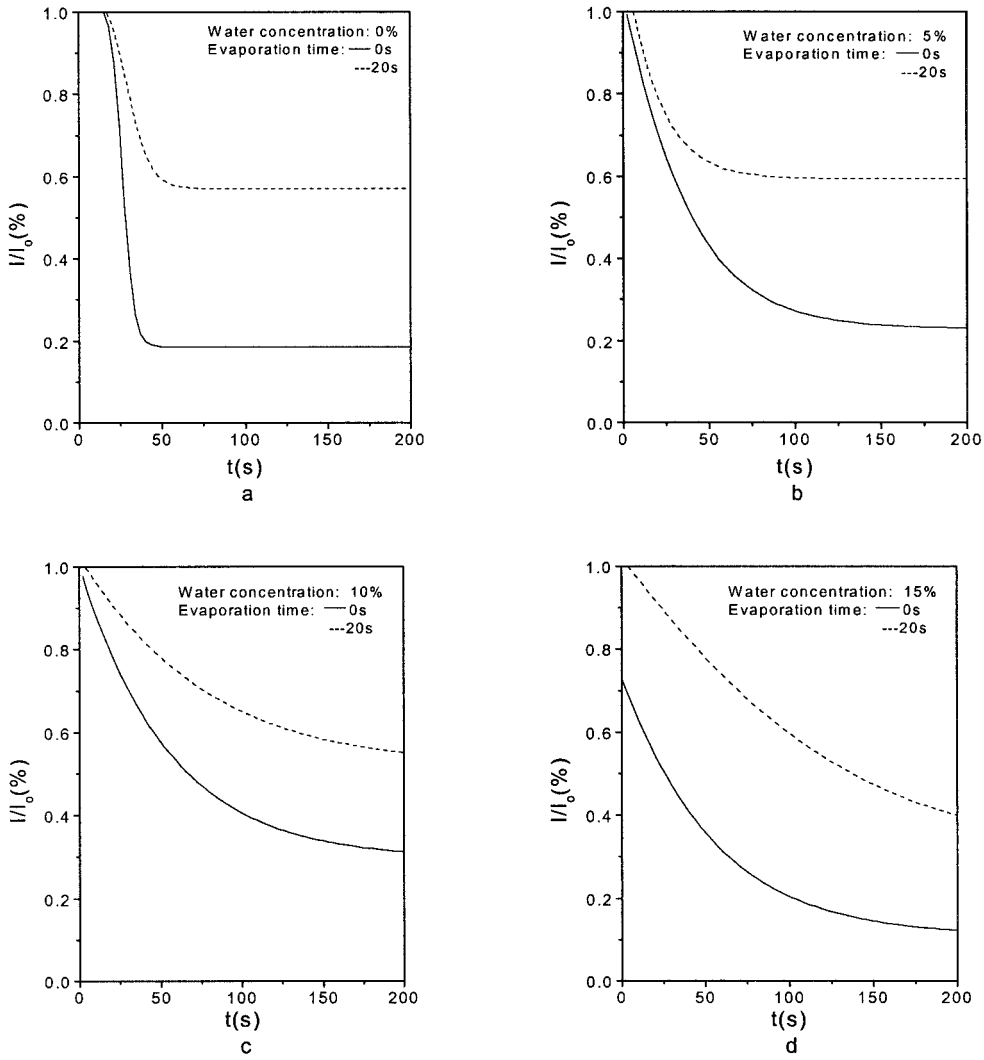

Figure 5 Light transmission–immersion time relationship for CA–acetone–water casting solution in a water coagulation bath.

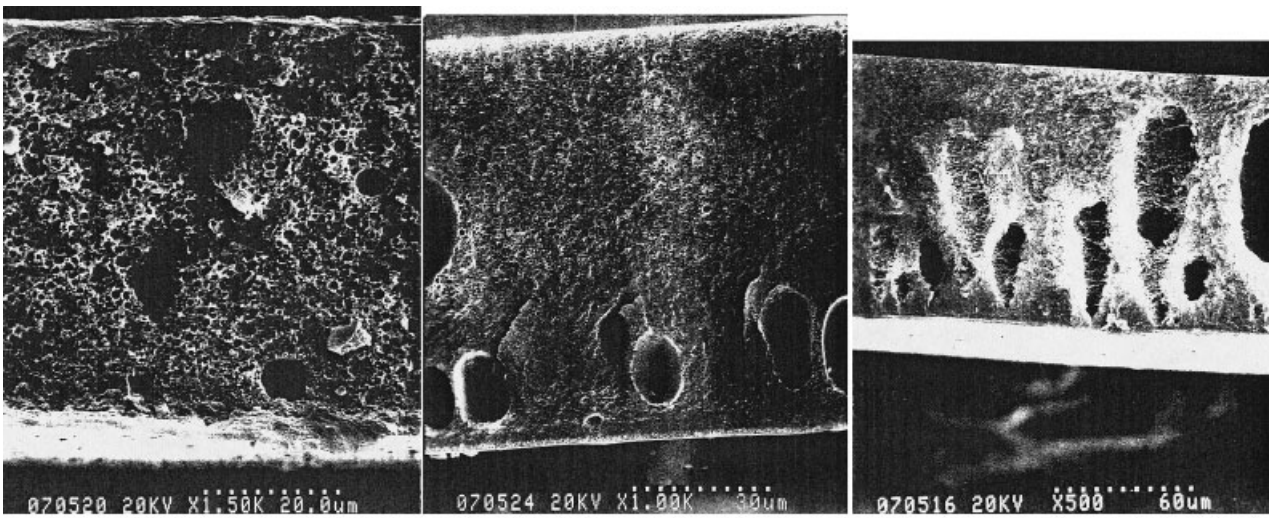

Figure 6 Whole cross-section structure of asymmetric CA membranes for different H_2O contents without evaporation (casting solution 25% CA): (a) water, (b) 5% water, and 15% water.

where t is the immersion time on the set of the cast membrane with the coagulation bath. The negative sign in the equation accounts for the fact that β decreases as t increases. β reflects the rate of solidifying of the cast membrane in the coagulation bath. The larger the β is, the faster the rate of solidifying of the cast membrane in the coagulation bath will be, which corresponds to the fast glass transition of the cast membrane and the loose morphological structure of the resulting membrane. The bigger β is, the more possible it is to bring on spinodal decomposition. The smaller β is, the easier it is to induce gelation transition of the cast membrane.

The minimum value of the light transmission intensity, denoted by I_{min}, is defined as the light transmission intensity when β is zero, which means that the phase separation has finished and the light transmission intensity through the membrane will not change with time anymore. I_{min} reflects the degree of dense or loose structure of the final membrane. When light transfers from one medium to another, it will spread in reflection and/or refraction if the internal structure of the medium is even. At this time, the rate of light transmission is only relative to the medium property itself. However, if there exist impurities and/or bubbles in the medium, light will spread in a diffuse reflection and/or diffuse refraction, which causes a part of light to be lost.[20] Hence, the more and the larger the internal pore of the cast membrane is formed during the phase separation, the weaker the intensity of light transmission through the membrane will be. Therefore, I_{min} can be used as an index to measure the degree of dense or loose structure in the membrane.

RESULTS AND DISCUSSION

CA concentration in the casting solution

The phase separation processes for CA–acetone casting solutions with different CA concentrations in a water coagulation bath all belonged to the delayed demixing, as shown in Figure 4. With an increase of CA concentration from 17 to 27.5%, the delayed demixing time increased from 9 to 15 s. According to Reuvers's explanation,[2,6,13] during the delayed time, there is a large outflow of solvent from the casting membrane solution, whereas the inflow of nonsolvent is relatively small.

Because of a net loss of solvent from the casting membrane, the CA concentration at the interface increased considerably. This concentration will reach a constant value as long as no demixing takes place and as long as the membrane can be treated as semiinfinite. Under these conditions, the thickness of the concentrated layer on the skin interface of the membrane increases with $t^{1/2}$, where t is the contact time between the CA casting membrane and the water coagulant. Only when the nonsolvent, water, has reached the other side of the membrane, can the local nonsolvent concentration in the membrane exceed the minimum value necessary for liquid–liquid demixing. In the sublayer, the CA concentration is increasing as well but to a lower extent. The concentrated layer hinders nonsolvent water diffusing into the sublayer. The diffusion rate of water into the sublayer will depend on the concentration of CA in the concentrated layer and sublayer, composition of the casting solution, the properties of coagulant, and so on.[4,14,15,17] If the concentration of CA in the concentrated layer is not high

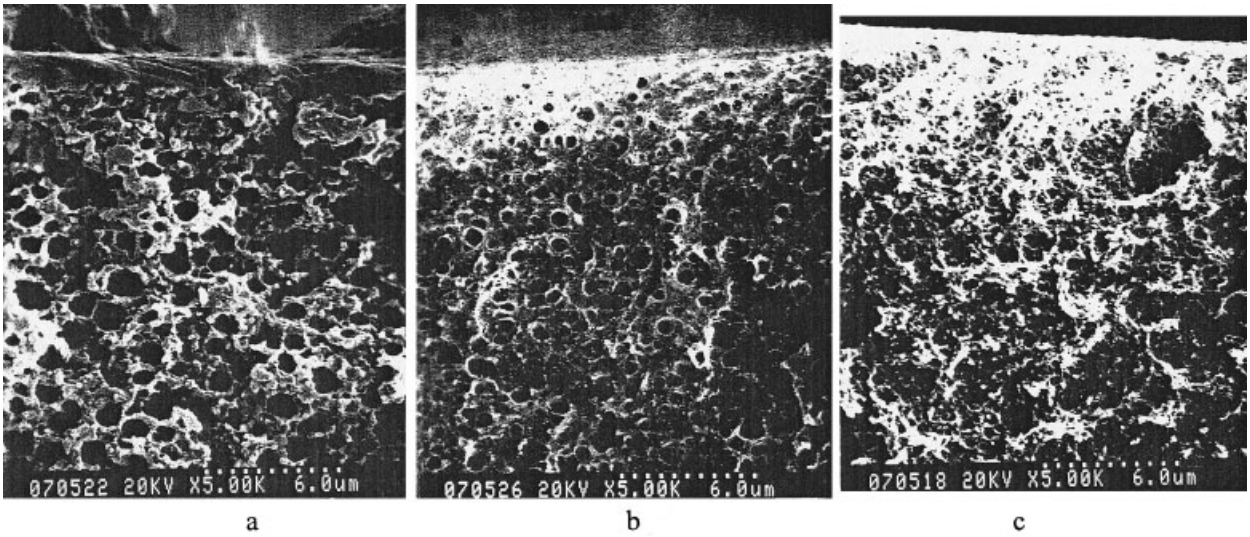

Figure 7 Partial cross-section structure of asymmetric CA membranes for different H_2O contents without evaporation (casting solution 25% CA): (a) water, (b) 5% water, and 15% water.

enough to hold back water diffusing into the sublayer and water itself has an ability to diffuse quickly through the concentrated layer, the phase separation process in the sublayer will not be controlled by the concentrated layer and will keep the phase separation characteristic of the original casting solution, spinodal decomposition, or nucleation and growth. However, when the CA concentration in the concentrated layer is concentrated high enough to hold the nonsolvent entering into the sublayer and limiting nuclei formation in the dilute CA phase or spinodal decomposition, the phase separation process in the sublayer will be slow, which will result in a closed-cell structure. So even under the condition of delayed demixing, different types of phase separation in the sublayer may appear. (See Table I.)

The light transmission technique was used to examine this process. Reuvers first made use of the light transmission–immersion time relationship to analyze the morphological structure of the membrane and thought that the liquid–liquid demixing process in polymer solutions during membrane formation may proceed in two different ways: delayed demixing and instantaneous demixing. The membranes from the instantaneous phase separation typically consist of a very thin but microporous skin layer and an open-cell finger or sponge support layer. The membranes from delayed phase separation result with a morphology comprising a dense and rather thick skin layer supported by a closed-cell sponge-like substructure.[2,6,13] Although Reuvers's work can predict membrane morphology, the instantaneous or delayed demixings themselves only represent the initial state of the phase separation. They do not reflect the whole process of phase separation from the onset of demixing to the total solidification of the membrane. Actually, phase separation is a process. Either the morphological structure in the surface or the structure in the sublayer formed and developed until the casting membrane was solidified completely. The light transmission technique itself monitored the whole process of the phase separation. Hence, we defined the other two new parameters: the rate of light transmission (β; or light transmission intensity) and the minimum light transmission intensity (I_{min}). These two parameters combining Reuvers's theory on the delayed and instantaneous demixings could monitor and reflect the whole process of the phase separation.

With an increase in CA concentration from 21 to 25%, the delayed time increased from 9 to 15 s. Ac-

TABLE II
Effect of the Evaporation Time[18,19]

Evaporation time (%)	Delayed demixing time (s)		CO_2/CH_4 selectivity		Permeability$(P/L)_{CO2} \times 10^5$ (cm^3/cm^2 s cmHg)	
	2.5% H_2O	10% H_2O	2.5% H_2O	10% H_2O	2.5% H_2O	10% H_2O
0	5	2	10.5	5.4	0.53	0.60
20	8	4	8.5	3.5	0.41	0.58
40			6.9	1.0	0.34	0.44
60			3.8		0.35	

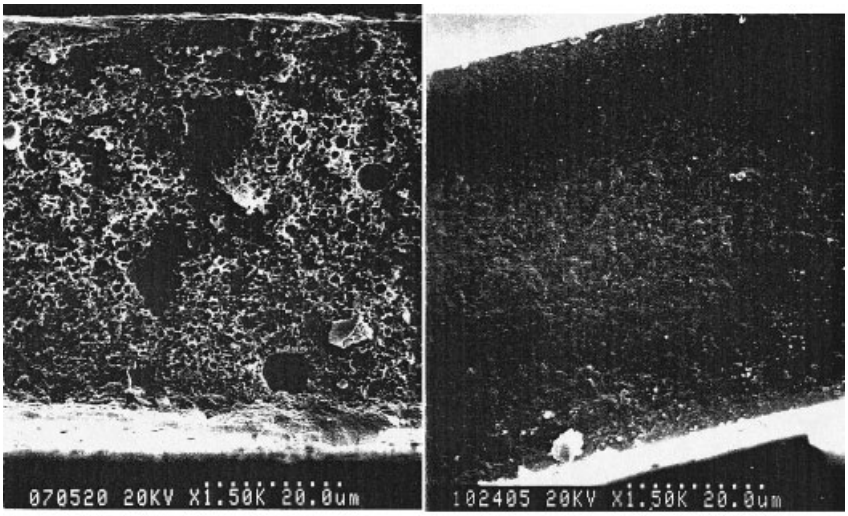

Figure 8 Whole cross-section structure of asymmetric CA membranes at different evaporation times (casting solution 25% CA): evaporation time (a) 0 s and (b) 40 s.

cordingly, the CO_2 selectivity of the membrane increased and the permeability of the membrane decreased. At the most instances, the results were coincident with the prediction by Reuvers's theory. The tendency of gradual decrease on I_{min} could explain the previous results further. However, it was difficult to explain the increase in CO_2 permeability from a CA concentration of 17% to a CA concentration of 21%, and the rapid increase of CO_2/CH_4 from a CA concentration of 25% to a CA concentration of 27.5% without any change of the delayed mixing time according to Reuvers's theory. We could explain this phenomena by rate of light transmission and minimum light transmission intensity.

When Figure 4(a) is compared with Figure 4(b), one can see that, although the total rate of light transmission in Figure 4(a) is faster than that in Figure 4(b), there exists the slower region of β after the delayed time in Figure 4(a). During this period, the interface layer was concentrated further so that the dense and thick transition layer under the skin was formed simultaneously, which resulted in the low CO_2 permeability at a CA concentration of 17%. Despite the same delayed time for CA concentrations of 25 and 27.5%, β in Figure 4(d) was much slower than that in Figure 4(c) just after the delayed time. The CA concentration at the interface layer in Figure 4(d) was much more concentrated during this period, which resulted in the double selectivity of CO_2/CH_4, even without any increase in delayed time.

Water concentration in the casting solution

For the ternary casting solution with the increase of H_2O content in the casting solution, the delayed time gradually became short, and the phase separation changed into instantaneous demixing. However, the pore sizes on the substructure of the membrane got smaller and denser. This was just because the rate of the light transmission became slower with the increase in H_2O content in the casting solution, as shown in Figures 6 and 7. When H_2O content in the casting solution was increased to 15%, larger finger-like pores appeared in the substructure. At this time, the minimum light intensity got lower once again.

Evaporation time

With the increase in the evaporation time, the delayed time increased, as shown in Figures 4 and 5(a,b), and the instantaneous demixing changed into delayed demixing, as shown in Figure 5(c,d). In many cases, the selectivity of the membrane increased, and the permeability of the membrane decreased. The separation performances and the corresponding structure of the membrane could be explained by Reuvers's theory. However, for some instances, the selectivity of the membrane decreased with an increase in evaporation time, as shown in Table II. The morphological structures of the membrane at different evaporation times are shown in Figure 8.

Reuvers's theory was unable to explain the previous results. However, with the increase in evaporation time, the rate of the light transmission became slower, and the minimum light intensity increased. This indicated that the substructure of the membrane became more dense and consisted of closed pores, which resulted in a large resistance to gas transport. According to Henis and Tripodi's resistance model, a large resistance to gas transport may result in a decrease in gas

selectivity even if the membrane has a dense top skin layer.[21,22]

Hence, the two new parameters, the rate of the light transmission and minimum light intensity could explain the many phenomena on the formation of the membrane by phase inversion. These two parameters, combining Reuvers's theory on instantaneous demixing and delayed demixing, can make full use of the light transmission–immersion time relationship and provide a convenient analytical method to predict the membrane morphologies.

We will report the further experimental results on the light transmission–immersion time relationship in future publications.

CONCLUSIONS

New parameters, light transmission rate and minimum light transmission, were proposed. These two parameters reflect the characteristics of the membrane-forming system and the formation process of the membranes by phase inversion. The relationship between the light transmission and the porous structure of the membrane can be explained by the geometrical optics principles.

The two parameters combining Reuvers's phase separation theory were used to explain the asymmetric CA membranes made at the different conditions. The light transmission–immersion time curves in the phase inversion process were successfully related with the morphological structure and separation performances of the correspondent membranes. The variation of the two parameters combining Reuvers's phase separation theory provides a convenient analytical method to initially predict membrane morphologies.

References

1. Frommer, M. A.; Messalem, R. M. Ind Eng Chem Prod Res Dev 1973, 12(4), 328.
2. Reuvers, B. Ph.D. Thesis, University of Twente, The Netherlands, 1987.
3. Tsay, C. S.; McHugh, A. J. J Polym Sci Part B: Polym Phys 1990, 28, 1327.
4. Pinnau, I.; Koros, W. J. J Polym Sci Part B: Polym Phys 1993, 31, 419.
5. Yilmaz, L.; McHugh, A. J. J Membr Sci 1986, 28, 287.
6. Reuvers, A. J.; van den Berg, J. W. A.; Smolders, C. A. J Membr Sci 1987, 34, 45.
7. Tsay, C. S.; McHugh, A. J. J Polym Sci Part B: Polym Phys 1991, 29, 1261.
8. Radovanvic, P.; Thiel, S. W.; Hwang, S. T. J Membr Sci 1992, 65, 231.
9. Hao, J. H.; Wang, S. J Appl Polym Sci, to appear.
10. Burghardt, W. R.; Yilmaz, L.; McHugh, A. J. Polymer 1987, 28, 2085.
11. Gaides, G. E.; McHugh, A. J. Polymer 1989, 30, 2118.
12. McHugh, A. J.; Tsay, C. S. J Appl Polym Sci 1992, 46, 2011.
13. Reuvers, A. J.; Smolders, C. A. J Membr Sci 1987, 34, 46.
14. van't Hof, J. A.; Reuvers, A. J.; Boom, R. M.; Rolevink, H. H. M.; Smolders, C. A. J Membr Sci 1992, 70, 17.
15. Pinnau, I.; Koros, W. J. J Appl Polym Sci 1991, 43, 1491.
16. Boom, R. M.; Wienk, I. M.; Van den Boomgaard, T.; Smolders, C. A. J Membr Sci 1992, 73, 227.
17. Hao, J. H.; Wang, S. J Appl Polym Sci 1998, 68, 1269.
18. Hao, J. H. Ph.D. Dissertation, Tianjin University, 1995.
19. Hao, J. H.; Wang, Z.; Wang, S. Polym Mater Sci Eng 1997, 13(4), 64 (in Chinese).
20. Zhang, Y. Applied Optics; Mechanic Industry Press: Beijing, 1982.
21. Henis, J. M. S.; Tripodi, M. K. U. S. Pat. 4,230,463 (1980).
22. Henis, J. M. S.; Tripodi, M. K. J Membr Sci 1981, 8, 233.